Engineering of self-assembled nanoparticle platform for precisely controlled combination drug therapy

Nagesh Kolishetti[a,b], Shanta Dhar[c], Pedro M. Valencia[d], Lucy Q. Lin[d], Rohit Karnik[e], Stephen J. Lippard[c,f,1], Robert Langer[b,c,f,1], and Omid C. Farokhzad[a,b,1]

[a]Laboratory of Nanomedicine and Biomaterials, Department of Anesthesiology, Brigham and Women's Hospital, Harvard Medical School, 75 Francis Street, Boston, MA 02115; [b]Massachusetts Institute of Technology-Harvard Center for Cancer Nanotechnology Excellence, [c]Departments of Chemistry, [d]Chemical Engineering, [e]Mechanical Engineering, and [f]Koch Institute for Integrative Cancer Research, Massachusetts Institute of Technology, 77 Massachusetts Avenue, Cambridge, MA 02139

Contributed by Robert Langer, August 10, 2010 (sent for review June 18, 2010)

The genomic revolution has identified therapeutic targets for a plethora of diseases, creating a need to develop robust technologies for combination drug therapy. In the present work, we describe a self-assembled polymeric nanoparticle (NP) platform to target and control precisely the codelivery of drugs with varying physicochemical properties to cancer cells. As proof of concept, we codelivered cisplatin and docetaxel (Dtxl) to prostate cancer cells with synergistic cytotoxicity. A polylactide (PLA) derivative with pendant hydroxyl groups was prepared and conjugated to a platinum(IV) [Pt(IV)] prodrug, *c,t,c*-$[Pt(NH_3)_2(O_2CCH_2CH_2COOH)(OH)Cl_2]$ [PLA-Pt(IV)]. A blend of PLA-Pt(IV) functionalized polymer and carboxyl-terminated poly(D,L-lactic-*co*-glycolic acid)-*block*-poly(ethylene glycol) copolymer in the presence or absence of Dtxl, was converted, in microfluidic channels, to NPs with a diameter of ~100 nm. This process resulted in excellent encapsulation efficiency (EE) and high loading of both hydrophilic platinum prodrug and hydrophobic Dtxl with reproducible EEs and loadings. The surface of the NPs was derivatized with the A10 aptamer, which binds to the prostate-specific membrane antigen (PSMA) on prostate cancer cells. These NPs undergo controlled release of both drugs over a period of 48–72 h. Targeted NPs were internalized by the PSMA-expressing LNCaP cells via endocytosis, and formation of cisplatin 1,2-d(GpG) intrastrand cross-links on nuclear DNA was verified. In vitro toxicities demonstrated superiority of the targeted dual-drug combination NPs over NPs with single drug or nontargeted NPs. This work reveals the potential of a single, programmable nanoparticle to blend and deliver a combination of drugs for cancer treatment.

chemotherapy | drug delivery | polymer-drug conjugate | targeting | temporal release

With a better understanding of the molecular underpinnings of cancer, it has become apparent that a single magic bullet target for treating the disease is a rare commodity (1, 2). Anticancer agents directed to an individual molecular entity frequently show limited efficacies, poor tolerability, and resistance profiles (3). Advances in our understanding of cell signaling pathways and mechanistic studies of existing drugs have identified synergistic therapeutic targets that may be concurrently utilized for more effective cancer treatments (3). Combination drug therapy is an attractive strategy, one that is used routinely to treat diseases like malaria (4), HIV/AIDS (5), diabetes (6), and cancer (3). Unlike single-agent chemotherapy, combination chemotherapy offers advantages such as signaling different pathways in cancer cells, maximizing therapeutic efficacy against individual targets, and overcoming mechanisms of resistance. Such combination therapy has the potential to improve the prognosis for a positive outcome, including the diminution of side effects. Therapeutic challenges when administering chemotherapeutic combinations include the choice of dosages to reduce side effects and the definitive delivery of the correct drug ratio and exposure to the targets of interest. These factors are very difficult to achieve when drugs are individually administered.

The development of nanotechnologies for effective delivery of multiple drugs or drug candidates in a temporally regulated manner to cancer cells can address these therapeutic challenges. Polymeric nanoparticle (NP) drug delivery vehicles have the ability to improve drug pharmacokinetics, biodistribution, cell- or tissue-specific targeting, and drug exposure kinetics, resulting in enhanced efficacy and improved tolerability (7–9). NPs comprised of poly(D,L-lactic acid-*co*-glycolic acid)-*block*-poly(ethyleneglycol) copolymer (PLGA-PEG) are especially promising as targeted drug delivery vehicles and confer the advantages of controlled drug release, enhanced stability, and the ability to carry a payload of thousands of drug molecules per NP vehicle (10–12). In addition, reactive functional groups can be incorporated at the polymer termini for further attachment of targeting moieties after NP formation (13–16). For example, our group utilized carboxyl-terminated PLGA-PEG to conjugate the A10 RNA aptamer, a targeting ligand that can recognize the prostate-specific membrane antigen (PSMA) on prostate cancer cells (15, 17). PSMA is highly expressed by virtually all prostate cancers (17–20) and the neovasculature of most nonprostate solid tumors including breast and lung cancers (21, 22). PSMA is currently the focus of several diagnostic and therapeutic clinical trials for prostate and nonprostate cancers (17–20, 23). Although PLGA-PEG NPs are effective at noncovalent encapsulation and subsequent release of hydrophobic drugs like docetaxel (Dtxl), the encapsulation of hydrophilic drugs may result in poor loading and drug encapsulation efficiency. Furthermore, although more than one hydrophobic drug can be encapsulated in a single PLGA-PEG NP, the noncovalent coencapsulation of more than one drug can result in batch-to-batch variability in drug load and release kinetics, especially when using drugs with varying solubility, charge, and molecular weight (12, 24–26). Compared to delivering a single drug through different coadministered NPs, the codelivery of multiple drugs via the same NP system has several advantages. These include definitive delivery of a correct ratio of each drug to the target of interest, synergistic therapeutic effects, suppressed drug resistance, and the ability to control drug exposure temporally. It is therefore important to develop a platform

Author contributions: N.K., S.D., S.J.L., R.L., and O.C.F. designed research; N.K., S.D., P.M.V., and L.Q.L. performed research; N.K., S.D., and P.M.V. contributed new reagents/analytic tools; N.K., S.D., P.M.V., R.K., S.J.L., and O.C.F. analyzed data; and N.K., S.D., P.M.V., S.J.L., and O.C.F. wrote the paper.

Conflict of interest statement: O.C.F. discloses his financial interest in BIND Biosciences and Selecta Biosciences, two biotechnology companies developing nanoparticle technologies for medical applications. BIND and Selecta did not support the aforementioned research, and currently these companies have no rights to any technology or intellectual property developed as part of this research. BIND and Selecta are biopharmaceutical companies founded by O.C.F. and R.L., where they both serve as members of the Board of Directors and Scientific Advisory Board.

[1]To whom correspondence may be addressed. E-mail: ofarokhzad@zeus.bwh.harvard.edu, rlanger@mit.edu, and lippard@mit.edu.

This article contains supporting information online at www.pnas.org/lookup/suppl/doi:10.1073/pnas.1011368107/-/DCSupplemental.

technology that allows for the precise control of combination drug therapy.

The present work describes the proof-of-concept demonstration of such a platform technology that simultaneously loads multiple chemotherapeutic drugs with distinct solubilities and modes of action inside a single polymeric NP. Using cisplatin (27–29) and Dtxl (30–35), two widely used Food and Drug Administration-approved chemotherapeutics with different solubility profiles, and prostate cancer as a model disease, we demonstrate targeted drug delivery to PSMA-expressing cells. First, a functionalized-poly(lactic acid) (PLA) polymer was synthesized and derivatized with platinum(IV) [Pt(IV)] prodrug pendants which, after reduction, release cisplatin. Next, a dual-drug delivery NP platform was assembled by blending carboxyl-terminated PLGA-PEG (PLGA-PEG-COOH) and Pt(IV)-modified PLA polymer [PLA-Pt(IV)] in a nanoprecipitation step to encapsulate Dtxl, resulting in NPs with high loading of hydrophilic Pt(IV) and hydrophobic Dtxl. The nanoprecipitation and NP formation can be achieved in bulk synthesis or using flow focusing in microfluidic channels, which can further automate the development of libraries of NPs with varying biophysicochemical properties carrying distinct drugs. In the final step, the NPs were surface functionalized with the A10 RNA aptamer, which binds to the extracellular domain of the PSMA for differential delivery of the NPs to prostate cancer cells. To examine the efficacy of the targeted NPs, we used LNCaP prostate epithelial cell line as a PSMA-expressing cell line and PC3 as a PSMA-negative control cell line (14, 15). The results of this study demonstrate the engineering and utilization of NPs having controlled release of the two commonly used cancer therapy drugs and their enhanced efficacy in prostate cancer cells. Our results provide a potentially important platform technology for spatiotemporal, controlled release of two or more drugs for future applications in human cancer chemotherapy.

Results and Discussion

Development of PLA-Pt(IV) Drug-Polymer Conjugate. To codeliver two or more therapeutic agents with varying physicochemical properties and to obtain adequate control over drug encapsulation and release, we synthesized a biodegradable polymer with reactive hydroxyl functional groups to enable the conjugation of various drugs to the polymer backbone (Scheme 1 and *SI Text*).

Specifically, the incorporation of reactive functional groups capable of forming ester bonds allows for the conjugation of distinct drugs, and the subsequent hydrolysis of this bond under physiological conditions can afford controlled drug release. Briefly, a biodegradable polylactide derivative with pendant hydroxyl groups (PLA-OH) was prepared via condensation copolymerization of lactic acid and 3-benzyloxy-2-hydroxypropionic acid (**2**) followed by deprotection of the benzyl groups, as shown in Scheme S1. This hydroxyl-functionalized polylactide can also be prepared by a ring opening copolymerization of lactide and 3-(benzyloxymethyl)-6-methyl-1,4-dioxozone-2,5-dione (**3**), as previously described (36, 37). The pendant functional groups provide a convenient handle for attaching different agents that could be utilized to construct NPs. For this study, the pendant hydroxyl functional groups of PLA-OH were conjugated with a succinic acid-derivatized Pt(IV) prodrug, *c*,*t*,*c*-[$Pt(NH_3)_2$-($O_2CCH_2CH_2COOH$)(OH)Cl_2] (**4**), to afford a cisplatin prodrug-functionalized polylactide, PLA-Pt(IV). The polymers, PLA-OH and PLA-Pt(IV), were characterized by using ^{1}H NMR spectroscopy (Fig. S1).

Conversion to hydroxyl-functionalized polylactide, PLA-OH, from PLA-OBn was visualized by a decrease in the intensity of phenyl rings at 7.3 ppm (Fig. S1). The presence of the platinum prodrug in PLA-Pt(IV) was visualized by the appearance of amine protons at 6.3 ppm in the NMR spectrum (Fig. S1) after conjugation with the prodrug. Atomic absorption spectroscopic (AAS) studies of the PLA-Pt(IV) confirmed that we were able to conjugate ~10 wt % platinum in the polymer. Attempts to increase the amount resulted in polymers that were not completely soluble in acetonitrile, chloroform, or tetrahydrofuran. Hence, for all the studies, the batch of ~10 wt% platinum-containing PLA-Pt(IV) was used.

Design and Synthesis of NPs. The design and preparation of the NPs is shown in Fig. 1. Synthesis of the NPs with PLGA-PEG was achieved by nanoprecipitation (14, 15). In nanoprecipitation, a diblock copolymer like PLGA-PEG is dissolved in a water miscible solvent (e.g., acetonitrile) and then added dropwise into an aqueous solution, generating NPs.

In general, by blending free PLA or PLGA with PLGA-PEG during NP synthesis, the resulting NPs are larger in size than those developed from PLGA-PEG only (38). In the current study, due to a presence of free PLA-Pt(IV), the sizes of the NPs obtained by conventional "bulk" nanoprecipitation were greater than 150 nm. NPs with smaller sizes are more effective at evading uptake by macrophages and remain longer in the bloodstream (24, 39, 40). We previously reported a microfluidic technology that enables reproducible preparation of distinct, homogeneous, PLGA-PEG NPs by rapid mixing through a method known as hydrodynamic flow focusing (HFF) (38). Furthermore, by simply varying the flow rates of different polymeric precursors into the microfluidic device, the properties of the resulting NPs can be systematically and reproducibly controlled, which presents an opportunity to develop a platform technology to rapidly synthesize libraries of distinct NPs. Hence, to reduce the size of the NPs, we employed HFF in which polymeric precursors in an organic solvent (i.e., acetonitrile) are mixed with an antisolvent (i.e., water) in a microfluidic device. This method enables rapid and homogeneous mixing of acetonitrile into water, resulting in the controlled nanoprecipitation of NPs. These NPs have smaller sizes and higher drug loading than those obtained from the bulk method (38). NPs prepared in the microfluidic devices had a size

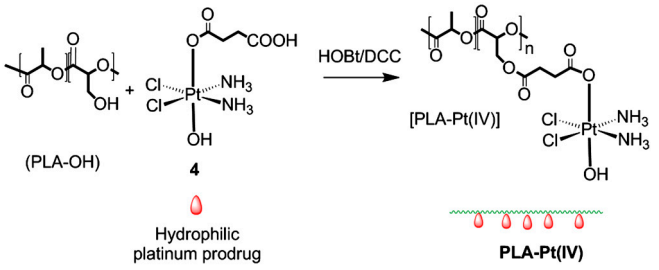

Scheme 1. Synthesis of PLA-Pt(IV) by coupling succinic acid-modified Pt(IV) prodrug with PLA-OH.

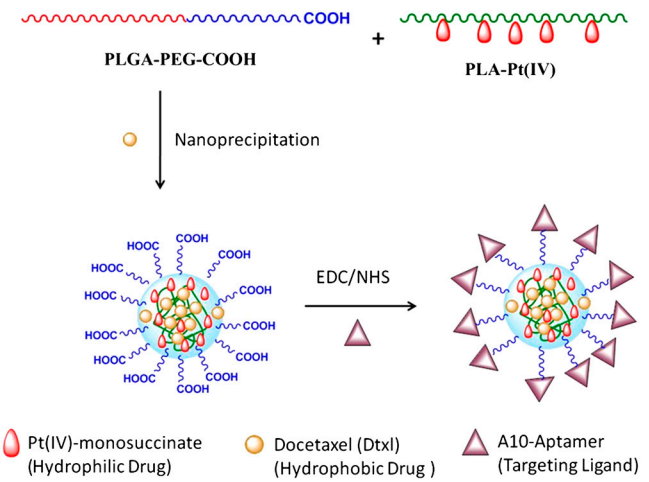

Fig. 1. Design and construction of NPs.

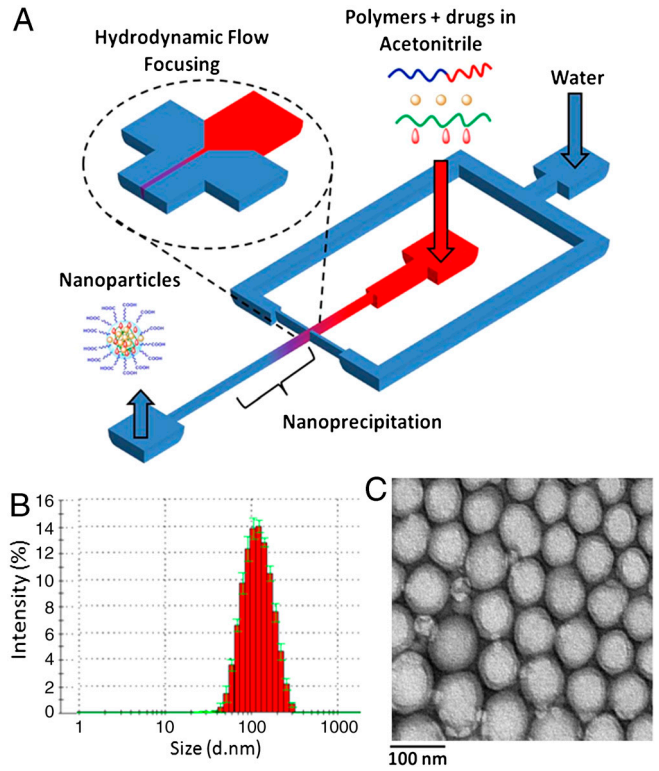

Fig. 2. Synthesis (*A*) and characterization of NPs via DLS (*B*) and TEM (*C*).

around 100 nm, even in the presence of free PLA-Pt(IV) (Fig. 2 and Table 1).

NPs obtained from microchannels using flow focusing were monodispersed (polydispersity index varied between 0.06–0.17) and had a diameter of ~100 nm as measured by dynamic light-scattering (DLS) and transmission electron microscopy (TEM) (Fig. 2 and Table 1). The polymer-drug conjugates had higher loading and encapsulation efficiency (EE) than the free drug (cisplatin or prodrug). An encapsulation efficiency of 95% or greater was obtained when 50 wt % of PLA-Pt(IV) or less was used during the nanoprecipitation process. When 5 mg of PLA-Pt(IV) and 5 mg of PLGA-PEG-COOH were used for nanoprecipitation, 5% loading and ~95% EE were obtained with respect to the hydrophilic platinum prodrug. Attempts to encapsulate free cisplatin or free Pt(IV) prodrug resulted in less than 0.5% loading and 5% EE, even with 2 mg of the free drug and 5 mg of PLGA-PEG-COOH. Similar to our previous studies, Dtxl loading of up to 1% was easily achieved with 80% EE (16, 25). Reproducible NP synthesis with high EEs and desired loadings were obtained with respect to hydrophilic and hydrophobic drugs in over 30 independent nanoprecipitation experiments.

In Vitro Release of Pt(IV) and Dtxl from NPs. Controlled release of the Pt(IV) and Dtxl from the NPs is an important prerequisite for success. For the release study, we dialyzed Pt(IV) and Dtxl-loaded NPs in 20 L of PBS, pH 7.4, at 37 °C using a 10 kDa cutoff membrane. The amount of Pt(IV) and Dtxl released from the NPs was measured, respectively, by AAS and HPLC. The controlled but temporally distinct release of Pt(IV) and Dtxl was observed from the profiles (Fig. 3), with Dtxl being released more rapidly than Pt(IV). This difference is expected because the former is noncovalently attached to the polymer, whereas the latter is covalently attached to the backbone, thus delaying its release from the NP. In PBS, ester hydrolysis is expected to be the predominant mode of platinum release, rather than reduction of Pt(IV) center. To confirm this expectation, a release study was performed in the presence of the reducing agent DTT (Fig. S2). A faster release of platinum was observed in the presence of DTT, supporting our hypothesis that Pt released in the absence of DTT is most likely in the +4 oxidation state. Together, these results demonstrate the ability of this system to supply drugs in a temporally controlled fashion by releasing one agent faster than the other. It is important to note that the release rates can be further tuned by varying the molecular weight of the polymer, as has been demonstrated for both Dtxl and cisplatin (16, 41).

Table 1. Characterization of NPs

	Size, nm	PDI*
NP	100	0.13
PLA-Pt-NP	93	0.06
PLA-Pt-(Dxtl)-NP	89	0.08
(Dxtl)-NP	112	0.17

*Polydispersity index.

Electrochemistry. The release of the active platinum(II) center is achieved by reduction of the platinum(IV) prodrug. PLA-Pt(IV) is redox-active and displays an irreversible cathodic wave in the cyclic voltammogram arising from the Pt(IV)/Pt(II) couple near −0.801 V vs. Ag/AgCl at pH 7.4. The corresponding value for the platinum-monosuccinate prodrug (**4**) is −0.850 V vs. Ag/AgCl (Fig. S3) under the same conditions. These values indicate that the presence of the polymeric backbone does not significantly influence the electronic or steric environment of the tethered platinum center and that this construct will effectively release active cisplatin required for anticancer activity. The low values of the cathodic peak for PLA-Pt(IV) also augurs well for the clinical requirement that this construct not be prematurely released in blood (42, 43).

Cytotoxicity Assays. We examined the basal cytotoxicity of NPs prepared by blending PLA-OH with PLGA-PEG (vehicle) using 3-(4,5-dimethylthiazol-2-yl)-2,5-diphenyltetrazolium bromide (MTT) assay. The IC_{50} of vehicle was 27 mg/mL, suggesting low in vitro cytotoxicity attributed to our polymer system (Fig. 4). Next we evaluated the cytotoxicities of PSMA targeted NPs made from blending PLA-Pt(IV) with PLGA-PEG (PLA-Pt-NP), which carry Pt(IV), and PLGA-PEG encapsulating Dtxl [(Dtxl)-NP], which provide Dtxl. The results were compared to those for NPs made by blending PLGA-PEG + PLA-Pt(IV) and encapsulating Dtxl [PLA-Pt-(Dtxl)-NP], which carry both Pt(IV) and Dtxl, to differentiate the cytotoxicity associated with Dtxl and Pt(IV) alone and any potential synergy that arises from dual delivery of these drugs. The PSMA targeting of NPs was achieved by utilizing the carboxylate group on the termini of PEG on the NP surface to attach the amine-terminated A10 aptamer via 1-ethyl-3-[3-dimethylaminopropyl]carbodiimide hydrochloride (EDC)/*N*-hydroxysuccinimide (NHS) chemistry (15, 25). These A10 aptamer-functionalized NPs bind to and are taken up by PSMA-

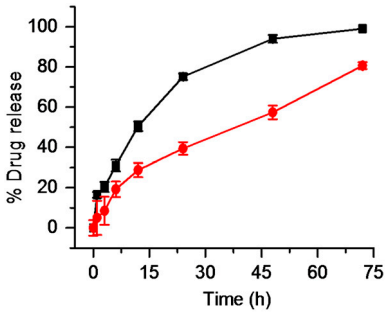

Fig. 3. In vitro release kinetics of encapsulated platinum (circle) and docetaxel (square) in PBS at 37 °C from NPs.

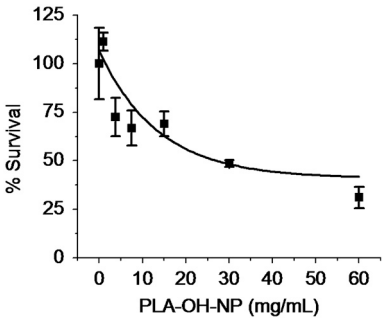

Fig. 4. In vitro toxicity of PLA-OH-NP.

expressing cancer cells through receptor mediated endocytosis, as previously described (15). The cytotoxicity of drug-loaded NPs against human prostate cancer LNCaP and PC3 cell lines was compared to free cisplatin and Pt(IV) prodrug (**4**), as summarized in Table 2. Comparison of the IC_{50} values suggests that PLA-Pt-NPs (~5 μM) have toxicity similar to that of cisplatin (~5 μM), whereas the targeted NPs are approximately 5 times more toxic to LNCaP cells (~0.95 μM), which express the PSMA protein. Because of the difference of more than two orders of magnitude in the IC_{50} values for **4** (~106 μM) vs. Dtxl (~0.3 μM) (44), we chose a Pt(IV) concentration 25 times higher than Dtxl for the cytotoxicity studies involving dual drugs. For dual delivery NPs, the targeted PLA-Pt-(Dtxl)-NP-Apt was more than twice as toxic as the nontargeted NP in LNCaP cells. On the other hand, there is no enhanced cytotoxicity with the targeted NPs in the PC3 cells, which do not express any detectable levels of PSMA. A comparison of these values (Table 2) indicates that PLA-Pt-(Dtxl)-NP is twice as effective in killing PSMA-expressing LNCaP cells than PLA-Pt-NP and (Dtxl)-NP, and 10 and 5.5 times more effective than PLA-Pt-NP-Apt and (Dtxl)-NP-Apt, respectively.

Interestingly, our data are different from previous reports where no synergistic effects occurred when free Dtxl and cisplatin were used for in vitro studies in the prostate cancer cells, suggesting that targeted codelivery may be an advantage (44).

Targeted Endocytosis of PLA-Pt-NP-Apt. Polymeric NPs can be taken up by cells through different processes, including phagocytosis and endocytosis. We carried out an immunofluorescence experiment to investigate the uptake of NPs. To investigate whether targeted NPs, PLA-Pt-NP-Apt, are taken up by PSMA-expressing LNCaP cells, we encapsulated a green fluorescent cholesterol derivative, 22-(N-(7-nitrobenz-2-oxa-1,3-diazol-4-yl)amino)-23,2,4-bisnor-5-cholen-3-ol) 22-NBD-cholesterol, within PLA-Pt-NP-Apt and visualized NP uptake after incubation with LNCaP cells by fluorescence microscopy.

As represented in Fig. 5, incubation of LNCaP cells with the cholesterol-coencapsulated PLA-Pt-NP-Apt for 1 h and the use of an early endosomal marker EEA-1 antibody resulted in the internalization of the NPs in the endosomes most likely through receptor mediated endocytosis, as previously described (15). Overlay of the fluorescence images obtained from FITC and Cy5 channels reveals early endosomal marker staining colocalized with NBD-cholesterol containing NPs, confirming endocytosis as the dominant mechanism for the uptake of these targeted NPs over the nontargeted PLA-Pt-NPs.

Table 2. Comparison of IC_{50} values with various NPs and drugs against LNCaP and PC3 cells as determined by the MTT assay

	IC_{50} in LNCaP cells, μM		IC_{50} in PC3 cells, μM	
	Pt conc.	Dtxl conc.	Pt conc.	Dtxl conc.
Prodrug (4)	106	—	36	—
Cisplatin	>5	—	9.9	—
PLA-Pt-NP	5	—	>10	—
PLA-Pt-NP-Apt	0.95	—	>10	—
PLA-Pt-Dtxl-NP*	0.22	0.009	0.2	0.008
PLA-Pt-Dtxl-NP-Apt*	0.09	0.0036	0.36	0.014
Dtxl-NP	—	0.1	—	0.01
Dtxl-NP-Apt	—	0.02	—	0.01

*[Pt] = 25 * [Dtxl]

Release of Cisplatin and Formation of Pt-d(GpG) Cross-Links. The anticancer activity of cisplatin stems from its ability to form cross-links with nuclear DNA. Several of these adducts have been structurally identified, of which the guanine–guanine intrastrand cross-link, *cis*-{$Pt(NH_3)_2d(GpG)$} represents >75% of total DNA platination. We used a monoclonal antibody, R-C18, specific for this adduct to investigate whether cisplatin released from PLA-Pt-NP-Apt forms this adduct with nuclear DNA. After 4 h incubation of LNCaP cells with PLA-Pt-NP-Apt, formation of the 1,2-d(GpG) intrastrand cross-links was observed by antibody-derived green fluorescence in the nuclei of these cells (Fig. 6).

Summary. In summary, this work demonstrates a versatile strategy for combination drug therapy with different biochemical properties with temporal control over their release. Attachment of a drug to the polymer backbone allowed for reproducible and tunable control over drug load in over 30 independent nanoprecipitation experiments, with ~95% EE, 5% loading of the hydrophilic Pt(IV) drug, and 80% EE, 1% loading of hydrophobic Dtxl. Targeted NPs with Dtxl and Pt(IV) showed superior efficacy over single drug NP analogues. The use of this polymer-drug conjugate approach for multiple drug delivery minimizes batch-to-batch variability of NPs during synthesis and has the potential for convenient adaptation to other therapeutic classes for treatment of human diseases where combination therapy is desired.

Materials and Methods

Cisplatin and *c,t,c*-$[Pt(NH_3)_2(O_2CCH_2CH_2COOH)(OH)Cl_2]$ (**4**) were prepared as previously described (45). *N,N*-dicylcohexylcarbodiimide (DCC), O-benzyl-L-serine, *p*-toluenesulfonic acid, sodium nitrite, NHS, EDC, paraformaldehyde, and *N,N*-diisopropylethylamine were purchased from Aldrich. PLGA with acid end groups was purchased from Adsorbable Polymers International. A PEG polymer of molecular weight 3,400 with a terminal amine and carboxylic group (NH_2-PEG-COOH) was custom synthesized (Nektar Therapeutics). PLGA-PEG-COOH was synthesized as previously described (14, 15). The A10 RNA aptamer with the sequence 5′-NH_2-spacer GGGAGGACGAUGCGGAUCAGCCAUGUUUACGUCACUCCUUGUCAAUCCUCAUCGGCiT-3′ containing 2′-fluoropyrimidines, a 3′-inverted T cap, and a 5′ amino group attached by a hexaethyleneglycol spacer was custom synthesized by RNA-TEC. ^{1}H NMR spectra were recorded on a Bruker AVANCE-400 NMR spectrometer with a Spectro Spin superconducting magnet in the Massachusetts Institute of Technology Department of Chemistry Instrumentation Facility. AAS measurements were taken on a Perkin Elmer AAnalyst 600 spectrometer. Dtxl quantification measurements were carried on Agilent HPLC using an RC18 column. Drug-encapsulated NPs were prepared by using the nanoprecipitation method. The NP size was obtained by quasi-electric laser light scattering by using a ZetaPALS dynamic light-scattering detector (15 mW laser, incident beam = 676 nm; Brookhaven Instruments).

Synthesis of PLA-Pt(IV). The strategy for the development of drug-functionalized polymers was based on a simple conversion of amino acids to their corresponding α-hydroxy acids (**2**) (Scheme S1). The first step involved conversion of the amine to a hydroxyl group via diazotization using sodium nitrite in the presence of an acid for 6 h (36, 37, 46). This high-yielding reaction provided the resultant monomer for direct use in condensation polymerization with lactic acid to give a polylactide copolymer, PLA-OBn (*SI Text*). The condensation polymerization was performed at 150 °C for 3 h with a continuous argon purge, followed by a further 3 h under vacuum. The same polymer was prepared using a ring opening polymerization of the cyclic lactide monomer (**3**), which was made by dehydration of the α-hydroxyl acid under very dilute conditions in toluene with 1% *p*-toluenesulfonic acid (36, 37, 46). The benzyl protecting group is necessary for avoiding side reactions of the hydroxyl group during the polymerization. The hydroxyl-functionalized biodegradable poly-

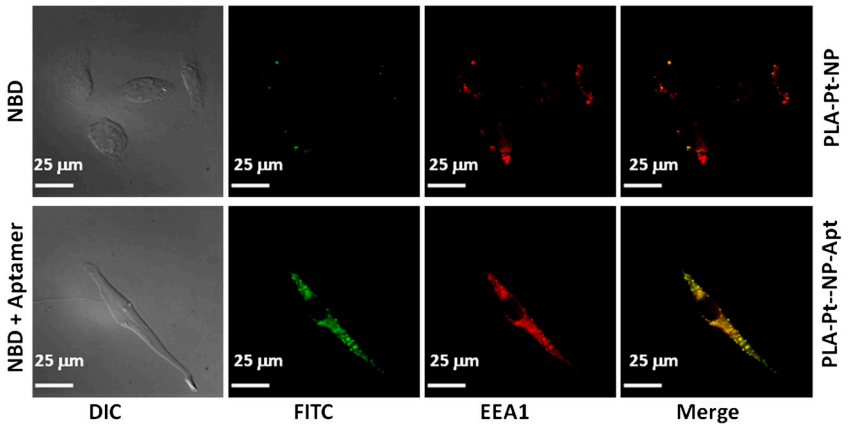

Fig. 5. Endocytosis of PSMA targeted NPs in LNCaP cells. Green fluorescent 22-NBD-cholesterol was coencapsulated in the PLGA-b-PEG nanoparticles and PSMA aptamers were conjugated to the surface of the particles. The early endosomes were visualized in red by using the early endosome marker EEA-1.

lactide (PLA-OH) was obtained by benzyl deprotection using a Pd/C catalyst at 50 psi pressure for 8 h (*SI Text*). Deprotection of the benzyl groups was confirmed by ^{1}H-NMR spectroscopy, monitoring the peak at 7.3 ppm. For the development of the biodegradable polymer with the pendant hydrophilic prodrug of cisplatin, platinum monosuccinate (45) **4** was conjugated with the polymer using DCC/hydroxybenzotriazole coupling for 12 h in dimethylformamide at room temperature to give PLA-Pt(IV) (Scheme 1 and *SI Text*).

Electrochemistry. Electrochemical measurements were made at 25 °C on a EG&G PAR Model 263 Potentiostat/Galvanostat with electrochemical analysis software 270 and a three electrode setup composed of a glassy carbon working electrode, a platinum wire auxiliary electrode, and an Ag/AgCl reference electrode. The electrochemical data were uncorrected for junction potentials. Tetrabutylammonium fluoride was used as a supporting electrolyte.

Synthesis and Characterization of NPs. NPs were made through nanoprecipitation in microfluidic channels (38). Briefly, a solution of PLGA-PEG (10 mg/mL) and PLA-Pt(IV) (10 mg/mL) in acetonitrile was run in the middle stream of a T channel at 5 μL/min, while water was run through the side streams of the channel at 50 μL/min. Dimensions of the channels were similar to the ones reported previously (38). In the case of the dual-drug-encapsulated NPs, Dtxl was also dissolved in acetonitrile and used during the encapsulation process. When the drug is not conjugated to the polymer, the NPs are labeled with drug name in parentheses. The resulting NP suspensions were purified by ultrafiltration using Amicon Ultracel 100 K membrane filters, washed thrice with water, and resuspended in DNAse/RNAse-free water. For the preparation of the A10 aptamer-targeted NPs, the NPs were treated with EDC/NHS and amine-modified A10 aptamer as reported earlier (14, 15). NP size was measured using both DLS and TEM. Samples for TEM were stained with 2% uranyl acetate and observed using a JEOL 2011 at 200 kV. Drug loading and EE were determined by quantifying the amount of drug in NP. Drug loading is defined as the mass fraction of drug in the nanoparticles, whereas EE is the fraction of initial drug that is encapsulated by the nanoparticles.

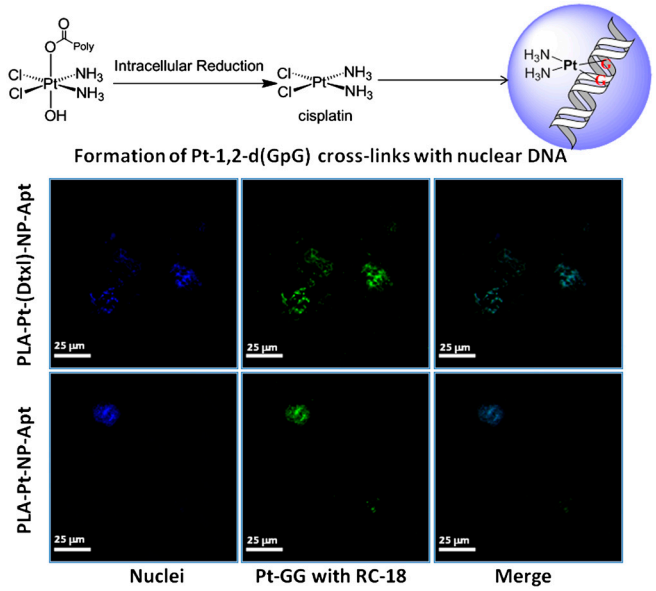

Fig. 6. Visualization of Pt-1,2,-d(GpG) intrastrand cross-links in the nuclear DNA of LNCaP cells after treatment with PLA-Pt-NP-Apt and PLA-Pt-(Dxtl)-NP-Apt. Nuclei were stained with Hoeshst (blue) and Pt-1,2-d(GpG) in DNA were visualized using Mab R-C18 (green).

Release of Platinum and Dtxl from the PLA-Pt-(Dtxl)-NPs. The suspension of PLA-Pt-(Dtxl)-NPs in water was aliquoted (100 μL) into several semipermeable minidialysis tubes (molecular weight cutoff 10 kDa; Pierce) and dialyzed against 20 L of PBS (pH 7.4) at 37 °C. At a predetermined time, an aliquot of the NP suspension was removed and dissolved in acetonitrile. The platinum content was determined by AAS, and the amount of Dtxl released was quantified by using HPLC.

Cytotoxicity Study. ***Cell line and cell culture.*** Human prostate cancer LNCaP and PC3 cells were obtained from the American Type Culture Collection. Cells were incubated at 37 °C in 5% CO_2 and grown in an RPMI medium 1640 supplemented with 10% FBS and 1% penicillin/streptomycin. Cells were passed every 3–4 d and restarted from the frozen stock upon reaching passage number 20.

MTT assay. The cytotoxic behavior of all the NPs was evaluated using the MTT assay. Solutions of the different NPs were freshly prepared in sterile PBS before use. Platinum and Dtxl content in the NPs were quantified by AAS and HPLC, respectively. Cells were seeded on a 96-well plate in 100 μL of RPMI medium 1640 and incubated for 24 h. The cells were then treated with different NPs at varying concentrations and incubated for 12 h at 37 °C. The medium was changed after 12 h, and the cells were further incubated for another 48 h. The cells were then treated with 20 μL of MTT (5 mg/mL in PBS) and incubated for 5 h. The medium was removed, the cells were lysed by adding 100 μL of DMSO, and the absorbance of the purple formazan was recorded at 550 nm using a microplate reader. Each well was performed in triplicate in three independent experiments for each cell line.

Fluorescence Imaging. ***Cell fixing solution.*** Paraformaldehyde (4.0 g) and NaOH (0.4 g) were dissolved in 100 mL of distilled water. To this solution, NaH_2PO_4 (1.68 g) was added and the pH was adjusted to be between 7.5 and 8.0 by adding NaOH.

Endocytosis study. To study the internalization of PLA-Pt-NP-Apt, we coencapsulated a green-fluorescing cholesterol derivative, 22-NBD-cholesterol. PLA-Pt-NP was used as a control to show the targeted uptake properties of our NP. LNCaP cells were seeded on microscope coverslips (1.0 cm) containing a confluence of 1×10^5 cells and grown overnight in a humidified incubator with 5% CO_2 at 37 °C in RPMI medium 1640. The medium was changed and a suspension of NBD-cholesterol-encapsulated-PLA-Pt-NP-Apt was added to a final fluorophore concentration of 10 μM. The cells were then incubated

for 1 h at 37 °C. The medium was removed and the cells were fixed using a 2% paraformaldehyde solution for 1 h at room temperature. After being washed three times with PBS (pH 7.4), the cells were then permeabilized with 0.1% Triton-X 100 in PBS for 10 min followed by five washes using PBS. The cells were then blocked with a blocking buffer (PBS, 0.1% goat serum, 0.075% glycin) for 30 min at room temperature. The cells were incubated for 1 h at 37 °C with an early endosomal marker, mouse monoclonal EEA-1, in a wet box according to the manufacturer-recommended procedure. After two washes with PBS, the cells were blocked with a blocking buffer for 30 min at RT and then incubated with the secondary Cy5 goat anti-mouse antibody for 1 h at 37 °C. After four washes with PBS and two washes with water, cells were mounted on microscope slides using the mounting solution [20 mM Tris (pH 8.0), 0.5% *N*-propyl gallate, and 70% glycerol] for imaging. Images were collected at 500 ms for both the FITC and Cy5 channels.

Detection of cisplatin 1,2-d(GpG) intrastrand cross-links. Detection of the platinum 1,2-d(GpG) cross-links was achieved by using an antibody specific to this adduct. Briefly, LNCaP cells were seeded in a six-well plate using RPMI medium 1640 and incubated overnight at 37 °C. Different NPs were then added to a final concentration of 20 μM and incubated at 37 °C. After 4 h, cells were trypsinized, washed with PBS, then resuspended in hydroxyethyl starch in isotonic sodium chloride solution sterile-PBS at a density of 1×10^6 per milliliter and placed onto a precoated slide (ImmunoSelect, Squarix) and air dried. Cell fixing was carried out at −20 °C in methanol for 45 min. Nuclear DNA was denatured by alkali (70 mM NaOH, 140 mM NaCl, 40% methanol vol/vol) treatment for 5 min at 0 °C. Cellular proteins were removed by a proteolytic procedure involving two steps. The cells were first digested with pepsin at 37 °C for 10 min and then with proteinase K at 37 °C for 5 min. After blocking with milk (1% in PBS, 30 min, 25 °C), slides were incubated with anti-(Pt-DNA) Mabs (R-C18 0.1 mg/mL in milk) overnight at 4 °C. After washing with PBS, immunostaining was performed by incubation with FITC-labeled goat anti-(rat Ig) antibody at 37 °C for 1 h. The nuclei of the cells were stained by using Hoechst (H33258) (250 μg/L) and mounted for imaging.

ACKNOWLEDGMENTS. We thank Dr. Jürgen Thomale, University of Duisburg-Essen Hufelandstr, Germany for a gift of the R-C18 antibody. We also thank Massachusetts Institute of Technology's Microsystems Technology Laboratory and staff for their help with device fabrication. P.M.V. thanks Fawziya Karim for assistance during experiments. This work was supported by National Cancer Institute Grants CA119349 (to O.C.F and R.L) and CA034992 (to S.J.L), the National Institute of Biomedical Imaging and Bioengineering Grant EB003647 (to O.C.F), and the David-Koch-Prostate Cancer Foundation Award in Nanotherapeutics (O.C.F and R.L). Electron microscopy image acquisition was performed in the Center for Material Science and Engineering imaging facility. P.M.V. is supported by the National Science Foundation graduate research fellowship.

1. Welch DR (1987) Biologic considerations for drug targeting in cancer patients. *Cancer Treat Rev* 14:351–358.
2. Strebhardt K, Ullrich A (2008) Paul Ehrlich's magic bullet concept: 100 years of progress. *Nat Rev Cancer* 8:473–480.
3. Jia J, et al. (2009) Mechanisms of drug combinations: Interaction and network perspectives. *Nat Rev Drug Discovery* 8:111–128.
4. Orjuela P, Gonzalez I, Osorio L (2004) Combination therapy as a strategy to prevent antimalarial drug resistance. *Biomedica* 24:423–437.
5. de Gaetano Donati K, Rabagliati R, Iacoviello L, Cauda R (2004) HIV infection, HAART, and endothelial adhesion molecules: Current perspectives. *Lancet Infect Dis* 4:213–222.
6. Suarez-Pinzon WL, et al. (2008) Combination therapy with glucagon-like peptide-1 and gastrin restores normoglycemia in diabetic NOD mice. *Diabetes* 57:3281–3288.
7. Brigger I, Dubernet C, Couvreur P (2002) Nanoparticles in cancer therapy and diagnosis. *Adv Drug Delivery Rev* 54:631–651.
8. LaVan DA, McGuire T, Langer R (2003) Small-scale systems for in vivo drug delivery. *Nat Biotechnol* 21:1184–1191.
9. Brannon-Peppas L, Blanchette JO (2004) Nanoparticle and targeted systems for cancer therapy. *Adv Drug Delivery Rev* 56:1649–1659.
10. Langer R (1998) Drug delivery and targeting. *Nature* 392(Suppl 6679):5–10.
11. Langer R (2001) Drug delivery: Drugs on target. *Science* 293(5527):58–59.
12. Zhang L, et al. (2008) Nanoparticles in medicine: Therapeutic applications and developments. *Clin Pharmacol Ther* 83:761–769.
13. Dhar S, Gu FX, Langer R, Farokhzad OC, Lippard SJ (2008) Targeted delivery of cisplatin to prostate cancer cells by aptamer functionalized Pt(IV) prodrug-PLGA-PEG nanoparticles. *Proc Natl Acad Sci USA* 105:17356–17361.
14. Farokhzad OC, et al. (2006) Targeted nanoparticle-aptamer bioconjugates for cancer chemotherapy in vivo. *Proc Natl Acad Sci USA* 103:6315–6320.
15. Farokhzad OC, et al. (2004) Nanoparticle-aptamer bioconjugates: A new approach for targeting prostate cancer cells. *Cancer Res* 64:7668–7672.
16. Gu F, et al. (2008) Precise engineering of targeted nanoparticles by using self-assembled biointegrated block copolymers. *Proc Natl Acad Sci USA* 105:2586–2591.
17. Lupold SE, Hicke BJ, Lin Y, Coffey DS (2002) Identification and characterization of nuclease-stabilized RNA molecules that bind human prostate cancer cells via the prostate-specific membrane antigen. *Cancer Res* 62:4029–4033.
18. Murphy GP, Elgamal AA, Su SL, Bostwick DG, Holmes EH (1998) Current evaluation of the tissue localization and diagnostic utility of prostate specific membrane antigen. *Cancer* 83:2259–2269.
19. Chang SS, et al. (1999) Five different anti-prostate-specific membrane antigen (PSMA) antibodies confirm PSMA expression in tumor-associated neovasculature. *Cancer Res* 59:3192–3198.
20. Ghosh A, Heston WDW (2004) Tumor target prostate specific membrane antigen (PSMA) and its regulation in prostate cancer. *J Cell Biochem* 91:528–539.
21. Morris MJ, et al. (2007) Phase I evaluation of J591 as a vascular targeting agent in progressive solid tumors. *Clin Cancer Res* 13:2707–2713.
22. Milowsky MI, et al. (2007) Vascular targeted therapy with anti-prostate-specific membrane antigen monoclonal antibody J591 in advanced solid tumors. *J Clin Oncol* 25:540–547.
23. Wright GL, Jr, et al. (1996) Upregulation of prostate-specific membrane antigen after androgen-deprivation therapy. *Urology* 48:326–334.
24. Alexis F, Pridgen E, Molnar LK, Farokhzad OC (2008) Factors affecting the clearance and biodistribution of polymeric nanoparticles. *Mol Pharmaceut* 5:505–515.
25. Cheng J, et al. (2007) Formulation of functionalized PLGA-PEG nanoparticles for in vivo targeted drug delivery. *Biomaterials* 28:869–876.
26. Chen H, et al. (2009) Coencapsulation of arsenic- and platinum-based drugs for targeted cancer treatment. *Angew Chem, Int Ed* 48:9295–9299.
27. Adelstein DJ, et al. (2010) Docetaxel, cisplatin, and fluorouracil induction chemotherapy followed by accelerated fractionation/concomitant boost radiation and concurrent cisplatin in patients with advanced squamous cell head and neck cancer: A southwest oncology group phase II trial (S0216). *Head Neck—J Sci Spec* 32:221–228.
28. Jamieson ER, Lippard SJ (1999) Structure, recognition, and processing of cisplatin-DNA adducts. *Chem Rev* 99:2467–2498.
29. Kelland L (2007) The resurgence of platinum-based cancer chemotherapy. *Nat Rev Cancer* 7:573–584.
30. Tankanow RM (1998) Docetaxel: A taxoid for the treatment of metastatic breast cancer. *Am J Health-Syst Ph* 55:1777–1791.
31. Kumar A, Wakelee H (2006) Second- and third-line treatments in non-small cell lung cancer. *Curr Treat Option Oncol* 7:37–49.
32. Thuss-Patience PC, Kretzschmar A, Reichardt P (2006) Docetaxel in the treatment of gastric cancer. *Future Oncol* 2:603–620.
33. Markman M (2007) New, expanded, and modified use of approved antineoplastic agents in ovarian cancer. *Oncologist* 12:186–190.
34. Khuri FR (2002) Docetaxel for locally advanced or metastatic non-small-cell lung cancer. Current data and future directions as front-line therapy. *Oncology* 16(Suppl 6):53–62.
35. Ajani JA, et al. (2007) Quality of life with docetaxel plus cisplatin and fluorouracil compared with cisplatin and fluorouracil from a phase III trial for advanced gastric or gastroesophageal adenocarcinoma: The V-325 study group. *J Clin Oncol* 25:3210–3216.
36. Leemhuis M, et al. (2006) Functionalized poly(α-hydroxy acid)s via ring-opening polymerization: Toward hydrophilic polyesters with pendant hydroxyl groups. *Macromolecules* 39:3500–3508.
37. Gerhardt WW, et al. (2006) Functional lactide monomers: Methodology and polymerization. *Biomacromolecules* 7:1735–1742.
38. Karnik R, et al. (2008) Microfluidic platform for controlled synthesis of polymeric nanoparticles. *Nano Lett* 8:2906–2912.
39. Buxton DB (2009) Nanomedicine for the management of lung and blood diseases. *Nanomedicine* 4:331–339.
40. Dobrovolskaia MA, Aggarwal P, Hall JB, McNeil SE (2008) Preclinical studies to understand nanoparticle interaction with the immune system and its potential effects on nanoparticle biodistribution. *Mol Pharmaceut* 5:487–495.
41. Avgoustakis K, et al. (2002) PLGA-mPEG nanoparticles of cisplatin: In vitro nanoparticle degradation, in vitro drug release and in vivo drug residence in blood properties. *J Controlled Release* 79:123–135.
42. Bell DN, et al. (2008) Comparitive protein binding, stability and degradation of satraplatin, JM118 and cisplatin in human plasma in vitro. *Clin Exp Pharmacol Physiol* 35:1440–1446.
43. Choi S, et al. (1998) Reduction and anticancer activity of platinum(IV) complexes. *Inorg Chem* 37:2500–2504.
44. Budman DR, Calabro A, Kreis W (2002) Synergistic and antagonistic combinations of drugs in human prostate cancer cell lines in vitro. *Anticancer Drugs* 13:1011–1016.
45. Dhar S, Daniel WL, Giljohann DA, Mirkin CA, Lippard SJ (2009) Polyvalent oligonucleotide gold nanoparticle conjugates as delivery vehicles for platinum(IV) warheads. *J Am Chem Soc* 131:14652–14653.
46. Noga DE, et al. (2008) Synthesis and modification of functional poly(lactide) copolymers: Toward biofunctional materials. *Biomacromolecules* 9:2056–2062.